

# Experimental Study on the Influence of Pore Structure and Group Evolution on Spontaneous Combustion Characteristics of Coal Samples of Different Sizes During Immersion

Zikun Pi,\* Rui Li, Wei Guo, Xiaoli Liu, Zhenya Zhang, Yan Wang, Yifu Zhang, Guangkuo Yin, and Xue Li



Cite This: *ACS Omega* 2023, 8, 22453–22465



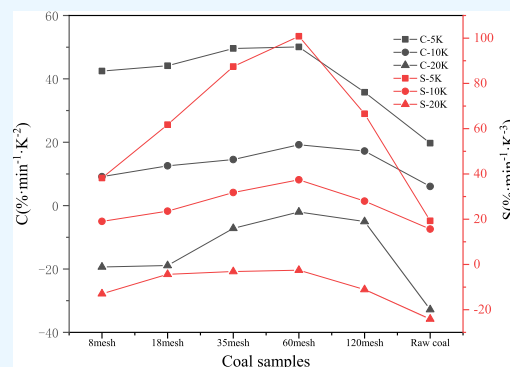
Read Online

ACCESS |

Metrics & More

Article Recommendations

**ABSTRACT:** To study the influence of water immersion on the evolution of the groups and spontaneous combustion characteristics of coal samples with different sizes, raw coal from the Fengshuigou Coal Mine operated by Pingzhuang Coal Company in Inner Mongolia was studied. The infrared structural parameters, combustion characteristic parameters, and oxidation reaction kinetics parameters of D1–D5 water immersion coal samples were tested, and the mechanism of spontaneous combustion during the oxidation of submerged crushed coal was investigated. The results were as follows. The water immersion process promoted the re-development of coal pore structure, and the micropore volume and average pore diameter were 1.87–2.58 and 1.02–1.13 times those of raw coal, respectively. The smaller the coal sample sizes, the more significant the change. At the same time, the water immersion process increased the contact point between the active group and oxygen in the coal, and the C=O, C–O, and  $-\text{CH}_3/-\text{CH}_2-$  groups in coal were further promoted to react with oxygen to generate  $-\text{OH}$  functional groups and improve the reactivity of coal. The characteristic temperature of water immersion coal was affected by the temperature rise rate, coal sample size, coal voidage, and other factors. Compared with the raw coal, the average activation energy of the water immersion coal with different sizes decreased by 12.4–19.7%, and the apparent activation energy of the coal sample with a size of 60–120 mesh was the lowest on the whole. In addition, the apparent activation energy in the low-temperature oxidation stage was significantly different.



## 1. INTRODUCTION

With the continuous development of coal mine mechanization, the intensity and depth of coal mining have increased, the influences of groundwater and water accumulation in the upper goaf have become increasingly serious, and the problem of the spontaneous combustion of coal has become more prominent.<sup>1,2</sup> In particular, the spontaneous combustion problem of water immersing coal needs to be solved urgently. Low-temperature oxidation of coal involves the release of heat, heat storage, rapid heating, eventually, and spontaneous combustion occurs.<sup>3</sup> This process is affected by many factors including environmental temperature, quality of the coal, oxygen supply conditions, coal particle size, and moisture content.<sup>4</sup> The spontaneous combustion and oxidation processes of coal are mainly manifested as changes in the functional group content, free radical concentration, and pore structure of the coal on the micro level and the changes in the thermal characteristics at the macro level.<sup>5</sup>

In actual production, for water preservation mining drainage,<sup>6</sup> unsealing of the fire area with water injection into the coal mining area is conducted,<sup>7</sup> and after the exploration

and release of old kiln water,<sup>8,9</sup> the water immersion coal is more likely to spontaneously ignite. Regarding research on the spontaneous combustion characteristics of the water immersion coal, many Chinese and foreign scholars have analyzed the influence of moisture on the physical and chemical structure and spontaneous combustion characteristics of coal from different perspectives. It is generally believed that the water immersion process dissolves the inorganic minerals and organic humus in the coal and increases the contact area between the active groups in the coal and oxygen.<sup>10–13</sup> In addition, water has a certain promotion effect on the formation of the water–oxygen complex, and the water–oxygen complex promotes reverse oxidation and spontaneous coal combustion.

Received: January 6, 2023

Accepted: May 26, 2023

Published: June 9, 2023



This is an important intermediate product in the process of spontaneous coal combustion.<sup>14–16</sup> Sensogut et al.<sup>17</sup> found that wet pulverized coal is more likely to spontaneously ignite than dry pulverized coal. Zhao<sup>18</sup> controlled the moisture content of coal samples in experiments and tested the spontaneous combustion tendency of coal samples. They concluded that there was an optimal moisture content, and the tendency of coal samples to spontaneously combust was the strongest at the optimal moisture content.

The water in coal needs to evaporate and absorb heat, and it also leads to significant changes in the physical and chemical structure of the coal. There are many methods of studying the pore structure of coal masses, which mainly include mercury injection,<sup>19,20</sup> transmission electron microscopy (TEM), nuclear magnetic resonance, carbon dioxide adsorption, nitrogen adsorption, and scanning electron microscopy (SEM) methods.<sup>21,22</sup> Choi et al.<sup>23</sup> found that the micropore volume of the water immersion air-dried coal was two times higher than that of the raw coal. Smith<sup>24</sup> and Dereppe<sup>25</sup> found that a larger pore size was the main channel involved in the reaction and gas generation. Fry<sup>26</sup> tested the swelling effect of the water immersion coal at room temperature and pressure and found that the volume swelling caused by water absorption was between 0.5 and 5%. In addition, they found that there was a linear relationship between the water absorption and swelling degree of coal. Song et al.<sup>27</sup> found through SEM, nitrogen adsorption, and electron spin resonance spectroscopy analyses that the longer the immersion time was, the larger the average pore size was, the higher the free radical concentration was, and the more likely the coal was to spontaneously ignite. Zhai et al.<sup>28</sup> conducted thermal characteristic analysis and infrared spectroscopy analysis of the water immersion bituminous coal and found that the relative content of the hydroxyl and carbonyl groups in the coal increased as the water immersion time increased. The water immersing process improved the indicated gas production of the water immersion coal, reduced the crossing point temperature of the water immersion coal, and increased the risk of the spontaneous combustion of the water immersion coal.<sup>29–31</sup> Zheng et al.<sup>32</sup> pointed out that as the number of active functional groups and the amount of heat released during oxidation of the water immersion air-dried coal increased, the activation energy decreased, and the spontaneous combustion tendency increased. In addition, thermokinetic analysis is considered to be a meaningful method of investigating the effect of water immersion on the spontaneous combustion mechanism. Especially, given the characteristics of coal with different particle sizes remaining in the goaf, there are few reports of the changes in the structure and the oxidation and spontaneous combustion characteristics of coal with different sizes through water immersion.

Thus, in this study, coal with different sizes was used to conduct water immersion experiments. The physicochemical structure, oxidation characteristics of the raw coal and water immersion coal samples with different sizes were compared to explore the spontaneous combustion and oxidation characteristics of coal with different sizes under water immersion. The results of this study provide a scientific basis for the prevention and control of the spontaneous combustion of the water immersion coal in the goaf of coal mines.

## 2. EXPERIMENTAL RESULTS AND DISCUSSION

### 2.1. Pore Structure Changes in Coal Samples before and after Immersion in Water.

The specific surface area,

pore volume, pore sizes, and other parameters of raw coal and water immersion coal samples of different sizes were measured through a low-temperature nitrogen adsorption experiment, as shown in Table 1. According to the results shown in Table 1,

**Table 1. Pore Structure Parameters of Raw Coal and Water Immersion Coal of Different Sizes**

coal sample	specific surface area (m <sup>2</sup> /g)	total pore volume (m <sup>3</sup> /g)	SF total micropore volume (m <sup>3</sup> /g)	BJH adsorption pore volume (m <sup>3</sup> /g)	mean hole diameter (nm)
D0	1.56825	0.00827	0.00033	0.009016	17.21320
D1	1.38234	0.00675	0.00062	0.006982	17.59843
D2	1.36887	0.00633	0.00063	0.006659	18.15348
D3	1.36697	0.00547	0.00066	0.005667	18.42327
D4	1.36028	0.00552	0.00072	0.005719	19.02989
D5	1.29851	0.00598	0.00085	0.006191	19.49281

the moisture content of the coal body decreased to about 85% of that of the raw coal under natural air drying of coal samples after water immersion. In the process of water immersion, inorganic matter and part of soluble organic matter in the raw coal were dissolved in water, ash content decreased, which was inversely proportional to the particle size of the water immersion coal. Some of the pores blocked by small organic molecules were cleared, and new micropores were generated. The micropore capacity of the water immersion coal was 1.87–2.58 times that of the raw coal. The smaller the size was, the more significant the micropore development was. Compared with the raw coal, the specific surface area of the water immersion coal decreased by 11.9–17.2% with the decrease in coal size. The total pore volume of the water immersion coal was only 66.1–81.6% that of the raw coal, which was proportional to the particle size of the water immersion coal. The average pore diameter of the water immersion coal was 1.02–1.13 times that of the raw coal, which was inversely proportional to the size of the water immersion coal. It shows that, in the process of immersion, the coal body absorbs water and expands, and the soluble substances in the tiny pores dissolve. In the drying process, some pores collapse, merge, and connect due to the action of pore surface shrinkage stress. The smaller the size of the coal sample, the more obvious the swelling effect and the more significant the effect of pore expansion.<sup>33</sup> This may be during the preparation process of coal samples, the grinding intensity of coal samples with large particle sizes were relatively small, which preserved more micropore structure. Meanwhile, the immersion process had a great influence on the micropore structure. Therefore, the total pore volume of coal samples with small particle size instead becomes smaller.

**2.2. Functional Group Changes in Coal Samples due to Water Immersion.** The spontaneous combustion and oxidation of coal are closely related to the types and contents of the active groups in the coal, and the surface of the coal sample contains a large number of active groups, mainly including oxygen-containing functional groups such as hydroxyl (–OH), carbonyl (C=O), carboxyl (–COOH), and methoxy (C–O) groups; and aliphatic hydrocarbons such as methyl (–CH<sub>3</sub>), methylene (–CH<sub>2</sub>–), and aromatic hydrocarbons (C=C). In the low-temperature oxidation of coal, the reactive groups in the coal react with molecular oxygen. Fourier transform infrared spectroscopy was conducted to obtain the FTIR spectra of coal samples, which

reflect the changes in the active groups in the coal according to previous research results on the molecular structure of the coal, as well as research results on coal chemistry and infrared spectroscopy. The spectral peaks of the main functional groups in the infrared spectrum of coal are listed in Table 2.

**Table 2. Spectral Peak Attribution of the Main Functional Groups in the Coal Infrared Spectra**

type	functional group	spectral peak position (cm <sup>-1</sup> )
oxygen-containing functional groups	-OH	3700–3610, 3550–3200, 1430–1350
	C=O	1690–1630, 1780–1715, 1880–1785
	C–O	1300–900
	-COOH	1715–1690, 2780–2350
aromatic hydrocarbons	C=C	1620–1430
aliphatic hydrocarbons	-CH <sub>3</sub> /-CH <sub>2</sub> -	2975–2945, 2940–2870, 2860–2850

The D1–D5 coal samples that had been immersed for 60 days and raw coal samples (D0) were directly heated to 110 °C under vacuum, and Fourier transform infrared spectroscopy was performed, the test results are shown in Figure 1. It can be

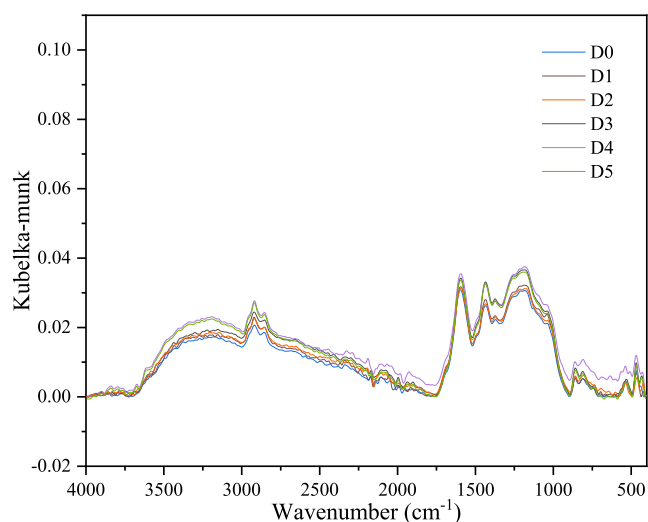


**Figure 1.** FTIR spectra of raw coal and water immersion coal samples with different particle sizes.

concluded that the overall trends of the infrared spectra of the water immersion coal samples with different sizes are the same. The corresponding positions of the peaks in the spectra are consistent. Compared with the raw coal sample, at wave numbers 1600–400 and 4000–1600 cm<sup>-1</sup>, the measured values of the raw coal sample are relatively small, but the changing trend and peak locations are also very similar. The changes in the active groups in the coal mainly occur in the 900–1880, 3000–2850, and 3700–3200 cm<sup>-1</sup> regions, which correspond to the oxygen-containing functional groups, aliphatic hydrocarbons, and hydroxyl structures, respectively.<sup>34</sup>

To further explore the changes in the active groups in the water immersion coal samples with different sizes, the Peakfit V4.2 software was used. After baseline correction and smoothing of the infrared spectrogram, the Gauss–Lorentz function was used to fit the peaks of the spectrum. Figure 2 shows the peak fitting curve of the D1 water immersion coal

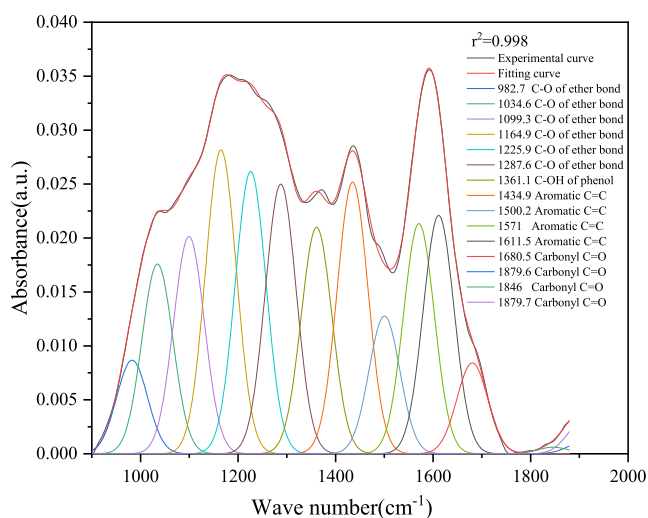


**Figure 2.** Peak fitting curves of the D1 water immersion coal samples for the 900–1880 cm<sup>-1</sup> region.

sample in the 1880–900 cm<sup>-1</sup> region. The confidence coefficient of the fitted curve is 0.998, the curve peaks represent phenol/alcohol/ether/ester (900–1330 cm<sup>-1</sup>), the hydroxyl group (1430–1350 cm<sup>-1</sup>), C=C stretching vibration in the aromatic ring or condensed ring (1430–1620 cm<sup>-1</sup>), and the carbonyl group (1785–1880, 1715–1870, and 1630–1690 cm<sup>-1</sup>). The other coal samples were also processed using the same peak fitting method, and the relative contents of the functional groups in the raw coal and saturated coal samples with different sizes after water immersion were obtained (Figure 3). The relative content of the ether bond (C–O) and

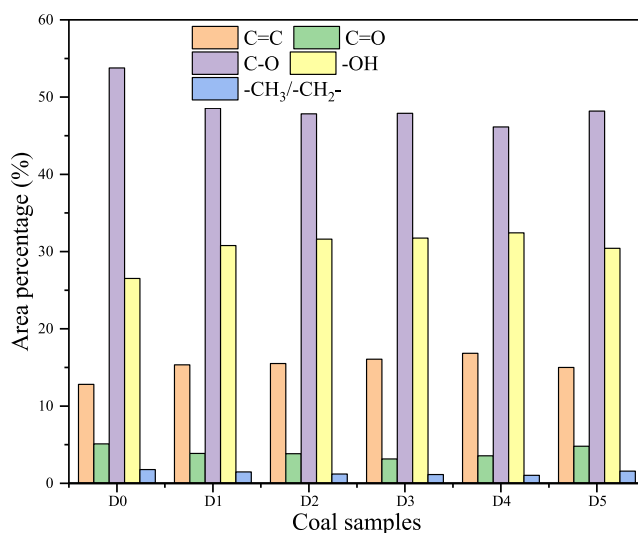


**Figure 3.** Relative contents of the functional groups in the raw coal and saturated coal samples with different particle sizes after water immersion.

hydroxyl group (-OH) in the experimental coal samples was relatively large, accounting for 72.3–80.6%. Compared with the raw coal samples, the content of the -OH and C=C groups in the water immersion coal samples with different sizes increased to varying degrees. As the size of the coal increased, the content initially increased and then decreased, with the maximum value occurring in the 60–120 mesh sample. In

addition, the content of the C=O, C–O, and –CH<sub>3</sub>/–CH<sub>2</sub>– groups in the coal samples decreased to varying degrees, exhibiting a trend of initially decreasing and then increasing with increasing size. This indicates that the water immersion process can increase the pore structure of the fractured coal body to a certain extent, which increases the contact sites between oxygen and the active groups in the coal; promotes the reaction between oxygen and the C=O, C–O, and –CH<sub>3</sub>/–CH<sub>2</sub>– groups in the coal; and generates –OH groups, and the proportion of the C=C functional group increases as the contents of other groups decrease.<sup>35</sup>

As is well known, during the infrared analysis of coal samples, any uncontrollable factors such as sample grinding, sample preparation thickness, and analysis time will affect the spectral peak area and intensity of the spectrogram to a certain extent. To avoid experimental errors caused by uncontrollable external factors, the peak area ratio was selected to fit the peaks of various functional groups, and the distribution characteristics of the functional groups in the coal samples were analyzed quantitatively. According to previous research results on infrared structural parameters,<sup>36</sup> the following three infrared structural parameters were used to characterize the changes in the water immersion coal samples with different particle sizes

$$\begin{cases} I_1 = \frac{A_{-\text{CH}_2-}}{A_{-\text{CH}_3}}, \\ I_2 = \frac{A_{\text{C-O}}}{A_{\text{C=C}}}, \\ I_3 = \frac{A_{\text{C=C}}}{A_{\text{C=O}} + A_{\text{C=C}}}, \end{cases} \quad (1)$$

where *A* is the peak area occupied by the functional groups (cm<sup>-1</sup>). *I*<sub>1</sub> is the length of the fat chain and the degree of branching in the coal. The larger the value of *I*<sub>1</sub> is, the longer the length of the fat chain in the coal is, and the less the branching chain is. *I*<sub>2</sub> is the ratio of the oxygen-containing functional groups to the aromatic hydrocarbons, and *I*<sub>3</sub> is the maturity of the coal.

The FTIR structural parameter values of the raw coal and coal samples with different particle sizes immersed in water are presented in Table 3. Compared with the raw coal, the *I*<sub>1</sub>

**Table 3. FTIR Structural Parameters of the Raw Coal and Saturated Coal Samples with Different Particle Sizes after Water Immersion Treatment**

coal samples	<i>I</i> <sub>1</sub>	<i>I</i> <sub>2</sub>	<i>I</i> <sub>3</sub>
D0	2.03	5.85	0.84
D1	1.54	3.56	0.86
D2	1.59	2.53	0.91
D3	1.51	2.50	0.91
D4	1.61	2.47	0.90
D5	1.65	2.94	0.90

values of the water immersion coal were only 62.6–77.0% of those of the raw coal. This shows that the water immersion process dissolved the soluble organic matter in the coal, loosened the structure of the coal, increased the content of the methyl component in the coal, increased the degree of branching, decreased the content of the methylene component, and shortened the length of the fat chain.<sup>37</sup> As the aliphatic

hydrocarbon content decreased, the structure of the raw coal became more stable than that of the water immersion coal, and the water immersion promoted the transformation of the stable components in the coal into unstable components.<sup>38</sup> As the size of the water immersion coal increased, the *I*<sub>1</sub> values decreased initially and then increased, and the coal samples with a particle size of 60–120 mesh had a minimum value; the main reason for this was that the smaller the size of the coal samples was, the more obvious the water immersing effect was, and more organic matter was dissolved. However, when the particle size of the coal samples was less than 60–120 mesh, the influence of water immersion and the small voidage of the coal samples prevent the organic matter from dissolving inside the coal body, resulting in an increase in the *I*<sub>1</sub> value.<sup>39</sup>

The *I*<sub>2</sub> values of the water immersion coal was 39.2–83.9% of that of the raw coal. As the particle size changed, the *I*<sub>2</sub> value fluctuates, but the fluctuation range was small. This indicates that the oxygen-containing functional groups such as the carbonyl group (C=O) and methoxy group (C–O) were removed from the coal samples during the water immersion process. In addition, the aliphatic hydrocarbons (–CH<sub>3</sub>/–CH<sub>2</sub>–) and some of the oxygen-containing functional groups in the molecular structure of the coal were connected to aromatic rings or other heterocycles through bridge bonds,<sup>40</sup> resulting in a decrease in the content of the oxygen-containing functional groups and an increase in the proportion of the C=C functional group with the decreasing content of other groups.

The *I*<sub>3</sub> values of the water immersion coal was 102.3–107.7% of that of raw coal. As the size increased, the *I*<sub>3</sub> value initially increased and then decreased. The *I*<sub>3</sub> value mainly reflects two processes of group deoxygenation and aromatization of coal samples.<sup>41</sup> The removal of the carbonyl group (C=O) and other groups in the coal, along with the increase in the degree of condensation and the consistency of the aromatic hydrocarbons, significantly enhances the vibration of the C=C in the skeleton of the coal, thus increasing the relative content of the aromatic hydrocarbons.<sup>42</sup>

### 2.3. Oxidation Characteristics and Kinetic Analysis of Coal Samples.

**2.3.1. Characteristic Parameters of Coal Sample Oxidation Reaction.** As is well known, the oxidation of coal exhibits a series of characteristic laws. From the macroscopic perspective, the main processes were the release of heat due to oxidation and the output of a variety of marker gases. From the microscopic perspective, the main processes were the change in the mesostructure and the active groups in the coal.<sup>43</sup> To explore the influence of the immersion process of coal samples with different particle sizes on the kinetic characteristics of the oxidation of coal, raw coal from Pingzhuang mine, the D0–D5 coal samples were selected for TG–DTG–DSC experiments, the TG–DTG–DSC curves are shown in Figures 4 and 5. As can be seen from Figure 4, the characteristic temperatures of the coal sample in the oxidation stage were obtained,<sup>44</sup> including the critical temperature *T*<sub>1</sub>, dry crack temperature *T*<sub>2</sub>, active temperature *T*<sub>3</sub>, maximum temperature of oxygen absorption and weight gain *T*<sub>4</sub>, ignition point temperature *T*<sub>5</sub>, and burnout temperature *T*<sub>6</sub>. The characteristic temperatures of coal samples for different heating rates are presented in Figure 4 and Table 4.

As can be seen from Figure 5, when the heating rate was 5, 10 K/min, the exothermic peaks of the water immersion coal samples appeared in advance, which were 423.73–429.42 and 442.24–447.01 °C, respectively. The extreme values of heat

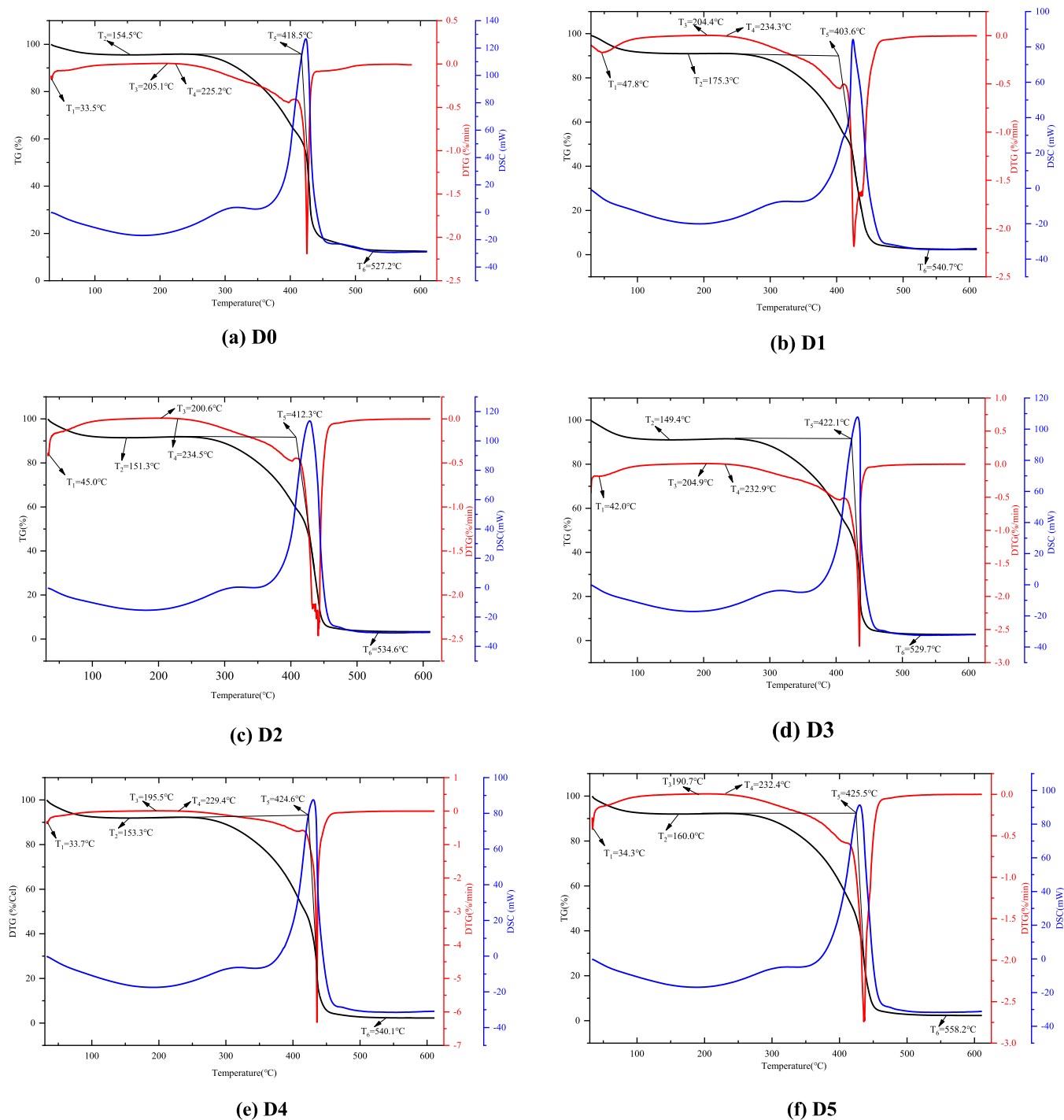


**Figure 4.** TG–DTG–DSC curves of the raw coal (D0) and water immersion coal samples (D1–D5) with heating rate of 5 K/min.

flow rate of the water immersion coal samples were higher than that of raw coal samples, which were 9.14–10.47, 10.31–13.29 W/g, respectively. Meanwhile, as the particle size increased, the extreme values of heat flow rate initially increased and then decreased, with a maximum value occurring for the 60–120 mesh sample. When the heating rate was 20 K/min, the exothermic peaks of the water immersion coal samples widened, the range of exothermic peaks were 465.89–475.14 °C, and the extreme values of heat flow rate were 9.19–11.17 W/g. As the particle size increased, the extreme values of heat flow rate initially increased and then decreased. This was mainly because with the heating rate increased, the rate of heat

gain of the coal accelerated, and the heating rate of the coal itself was accelerated. However, hindered by the oxygen supply conditions, some of the active groups could not react in time, resulting in a lag in the oxidation reaction. In addition, the exothermic characteristics of coal samples with different particle sizes changed significantly, and the calorific value were higher than raw coal. This further indicated that the risk of spontaneous combustion of water immersion coal in goaf was higher.

As can be seen from Figure 4 and Table 4, in the water loss and weight loss phase ( $T_1$ – $T_2$ ), the critical temperature ( $T_1$ ) of the water immersion coal sample was greater than that of

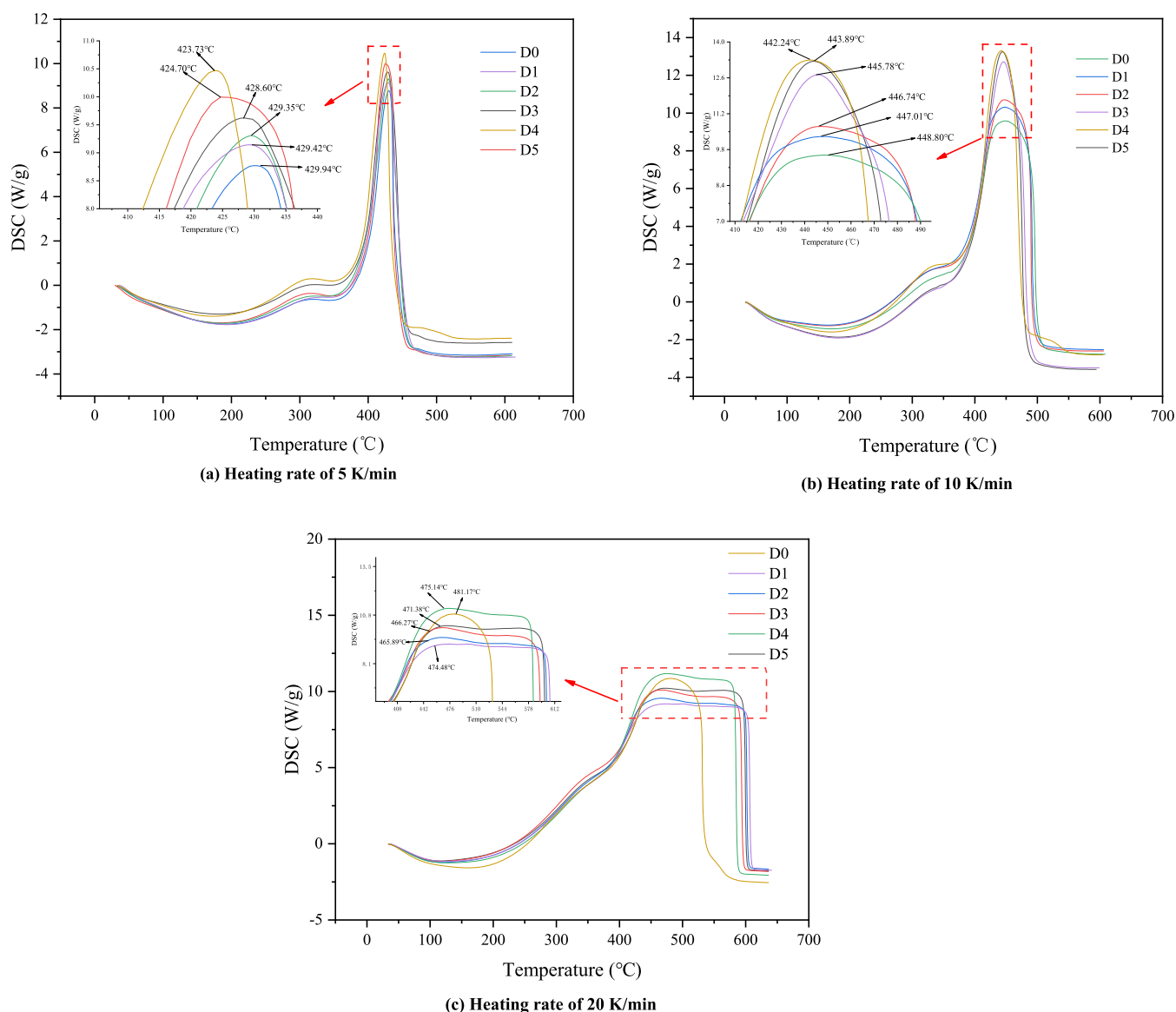


**Figure 5.** DSC curves of the raw coal and water immersion coal samples for different heating rates.

**Table 4.** Characteristic Temperatures of the Raw Coal and Water Immersion Coal Samples for Different Heating Rates

rate of heating ( $\text{K} \times \text{min}^{-1}$ )	coal sample	characteristic temperature ( $^{\circ}\text{C}$ )					
		$T_1$	$T_2$	$T_3$	$T_4$	$T_5$	$T_6$
10	D0	52.8	168.1	213.4	245.4	475.9	530.1
	D1	56.3	190.4	209.0	230.8	427.2	544.7
	D2	54.2	185.0	212.0	238.5	422.7	545.5
	D3	65.3	178.6	209.8	234.7	411.5	547.9
	D4	64.1	177.9	208.5	229.3	461.8	550.5
	D5	63.9	179.8	213.1	235.0	489.4	543.1
20	D0	57.7	179.2	223.7	231.0	495.3	531.4
	D1	77.5	188.9	214.8	243.1	473.9	599.3
	D2	81.0	178.7	214.9	236.8	477.6	593.6
	D3	81.7	197.1	216.0	233.9	466.0	601.8
	D4	83.0	192.9	213.9	239.4	490.1	584.8
	D5	78.7	196.3	207.6	250.7	515.3	578.9

the raw coal sample, as the heating rate increased, the critical temperature  $T_1$  gradually exceeded that of the raw coal. In addition, as the particle size and heating rate increased, the  $T_1$  values increased gradually and showed a fluctuation pattern.

This was mainly because the moisture content of the water immersion coal sample and the content of the hydroxyl ( $-\text{OH}$ ), aromatic hydrocarbons ( $\text{C}=\text{C}$ ), and other groups were higher than those of the raw coal samples, which were

**Table 5. Flammability Index and Composite Combustion Index of the Raw Coal and Water Immersion Coal Samples for Different Heating Rates**

combustion performance parameters	rate of heating (K × min <sup>-1</sup> )	coal samples					
		D0	D1	D2	D3	D4	D5
flammability index ×10 <sup>9</sup> (% min <sup>-1</sup> ·K <sup>-2</sup> )	5	19.70442	42.48495	44.144	49.5819	50.0662	35.76248
	10	6.05548	9.15073	12.56604	14.53905	19.20436	17.22915
	20	-32.82975	-19.35977	-18.89809	-7.17354	-2.01093	-5.03244
composite combustion index ×10 <sup>12</sup> (% min <sup>-2</sup> ·K <sup>-3</sup> )	5	19.26298	38.21	61.75556	87.42357	100.82751	66.5705
	10	10.63066	19.04501	23.54092	31.772	35.39669	23.97649
	20	-24.08936	-12.94442	-4.37014	-3.14132	-2.51547	-11.06107

affected by the evaporation and water loss from the water immersion coal samples and the gas desorption during this stage. The most significant change was observed for the coal samples with a particle size of 60–120 mesh. This was mainly because when the particle sizes of the coal sample were small, the specific surface area and pore capacity of the coal sample were small, but the average pore sizes of coal samples were larger, and oxygen moves more freely through the pores. However, when the particle sizes were too small, the void ratio of the coal sample was reduced, which led to difficulty in transporting the products of the oxidation reaction and hindered the entry of external oxygen. Therefore, the total oxidation reaction rate was relatively small.<sup>45</sup> This indicates that the oxidation dehydration and desorption processes of the coal sample at low temperatures were affected by factors such as water content, heating rate, relative surface area, average pore size, and void ratio.

In the dynamic equilibrium stage ( $T_2$ – $T_3$ ),<sup>46</sup> the dry cracking temperature ( $T_2$ ) of the water immersion coal sample was greater than that of the raw coal sample, while the active temperature ( $T_3$ ) was lower than that of the raw coal sample. As the particle size increased, the dry cracking temperature initially decreased and then increased, with a minimum value occurring for the 35–60 mesh sample, while the active temperature initially increased and then decreased, with a maximum value occurring for the D4 sample. This was mainly due to the immersion process of the coal sample, which improved the moisture content of the coal sample. In addition, the particle size of the coal sample also had a certain impact on the drying and cracking temperature. The water immersion process also caused the C=O, C–O, and –CH<sub>3</sub>/–CH<sub>2</sub>– groups in the coal to react with oxygen to form functional groups such as –OH and C=C, which increased the active groups in the coal, reduced the time it took for the dynamic equilibrium of the previous stage to be broken, and reduced the active temperature.

During the oxygen gain phase ( $T_3$ – $T_4$ ), the  $T_4$  values of the water immersion coal samples were greater than those of the non-water immersion raw coal samples. As the heating rate increased, the  $T_4$  value of the maximum temperature of the oxygen absorption and weight gain remained unchanged; and as the particle size of the water immersion coal sample increased, the  $T_4$  value also remained unchanged. This was mainly because water immersion increased the content of the active groups in the coal, increasing the oxidation reaction rate of the water immersion coal samples. After the temperature of the water immersion coal sample increased to the active temperature, with the continuous increase in temperature, the weight of the coal sample increased during this process

through the chemical adsorption of oxygen. When the temperature reached  $T_4$ , the coal molecules in the coal sample reached the temperature and energy critical points of macromolecular ring fracture and decomposition. This process was independent of the specific particle size of the coal sample.

In the thermal decomposition stage ( $T_4$ – $T_5$ ), when the heating rate was 5 K/min, as the particle size of the water immersion coal decreased, the ignition point temperature  $T_5$  gradually exceeded that of the raw coal; however, when the heating rate was 10, 20 K/min, the  $T_5$  values of the water immersion coal samples were all smaller than those of the non-water immersion raw coal samples. As the heating rate increased, the ignition point temperature  $T_5$  also increased; and as the particle size of the water immersion coal increased, the  $T_5$  value initially decreased and then increased, with the minimum value occurring for the D4 sample. This was mainly because water immersion increased the content of the active groups in the coal, especially the content of the hydroxyl group, which increased the low-temperature oxidation rate of the water immersion coal, thus increasing the  $T_5$  value of the water immersion coal. As the heating rate increased, the rate of heat gain of the coal accelerated, and the heating rate of the coal itself was accelerated. However, hindered by the oxygen supply conditions, some of the active groups could not react in time, resulting in a lag in the oxidation reaction.<sup>47</sup> In addition, due to the increase in the heating rate during this stage, the temperature at which the active groups in the coal started to participate in the reaction also increased, thus increasing the value of  $T_5$ . As a result, the reaction rate of the coal with oxygen was affected by the pore structure, active group content, oxygen supply, and gas exchange conditions.

During the combustion phase ( $T_5$ – $T_6$ ), the burnout temperatures ( $T_6$ ) of the water immersion coal samples were greater than those of the non-water immersion raw coal samples. As the heating rate increased, the  $T_6$  value increased. As the particle size of the coal increased, the  $T_6$  value initially decreased and then increased. This indicates that water immersion played a role in promoting the coal oxidation reaction to a certain extent, and it caused the coal to burn faster. As a result, the burnout temperature increased, the coal could be further fully burned, and the heat released from the water immersion coal increased.

In combination with the changes in infrared structural parameters of coal samples with different sizes (Table 3), infrared structural parameters  $I_1$ ,  $I_2$ , and  $I_3$ , coal particle size  $P_s$ , heating rate  $H_r$ , and characteristic temperature  $T_5$  were analyzed using the least square method and stepwise regression analysis. The functional relationship was obtained using the SPSS software:  $T_5 = 4.35H_r + 79.02I_2 + 4.06P_s \cdot I_2 - 6.42P_s +$

266.95, and the correlation coefficient  $R^2$  was 0.936. It can be seen that the ignition point temperature of coal samples with different sizes was mainly affected by the Hr, Ps, and oxygen-containing functional groups.

**2.3.2. Combustion Characteristic Parameters of Coal Samples.** As important indices for evaluating the combustion intensity of coal, the combustion characteristics have been widely used in the study of the mixed combustion of coal and other substances and the preparation of flame-retardant materials for coal.<sup>48</sup> To further understand the variations in the combustion performance of the water immersion coal samples with different particle sizes, the flammability index<sup>49</sup> and comprehensive flammability index<sup>50</sup> were analyzed. The specific calculation for these indices is shown in the following equation, and the combustion performance parameters of the raw coal and water immersion coal samples under different heating rates are shown in Table 5 and Figure 6

$$\begin{cases} C = \frac{(dw/dt)_{\max}}{T_i^2}, \\ S = \frac{(dw/dt)_{\max}(dw/dt)_{\text{mean}}}{T_i^2 \cdot T_h} \end{cases} \quad (2)$$

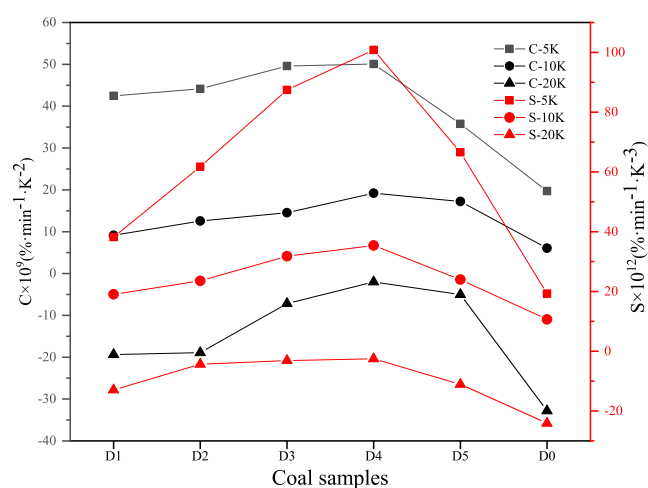


**Figure 6.** Combustion performance parameters of the raw coal and water immersion coal samples for different heating rates.

where  $C$  is the flammability index ( $\% \cdot \text{min}^{-1} \cdot \text{K}^{-2}$ ),  $(dw/dt)_{\max}$  is the maximum mass loss rate ( $\%/ \text{min}$ ),  $T_i$  is the ignition temperature (K),  $S$  is the composite combustion index ( $\% \cdot \text{min}^{-1} \cdot \text{K}^{-3}$ ),  $(dw/dt)_{\text{mean}}$  is the average combustion rate ( $\%/ \text{min}$ ), and  $T_h$  is the burnout temperature (K).

It can be seen from Figure 6 that the experimental heating rate had a large influence on the low-temperature oxidation rate of coal samples. As the heating rate increased, overall, the coal samples exhibited thermal hysteresis.<sup>51</sup> This was mainly because when the heating rate was too fast, the temperature difference between the inside and outside the coal sample increased, which hindered the evolution and precipitation of the volatile substances inside the coal sample and, thus, affected the combustion of the coal. The combustion time of the volatile substances was prolonged, and the environmental oxygen supply rate was also hindered, which further affected the burning of the coal. As the particle size increased, the flammability index and comprehensive combustion index of

the water immersion coal samples initially increased and then decreased, with the maximum value occurring for the D4 sample, which was greater than that of the raw coal samples. This shows that water immersion promoted the low-temperature oxidation of coal, and the flammability and comprehensive combustion characteristics of the water immersion coal were improved.

When the heating rate was 5 K/min, it may be because the temperature difference between inside and outside the coal sample was small, and the material exchange channel between inside and outside the coal sample was less affected by the temperature difference between inside and outside. Moreover, with the increase of coal particle sizes, the specific surface area and pore capacity of the coal sample increased, but the average pore diameter decreased. Meanwhile, it was also comprehensively affected by the moisture content and voidage ratio of the coal sample. The coal sample had a better oxidation combustion effect, so the comprehensive combustion characteristics index,  $S$ , shows a trend of rapid increase and rapid decrease, and with the maximum value occurring for the D4 sample, the value of  $S$  was 2.6 times that of the raw coal. When the heating rate was 20 K/min and the coal particle size was larger than 18–35 mesh, the temperature difference between inside and outside of the coal sample was significant. Meanwhile, although the specific surface area and pore capacity of the coal sample were larger, the pore size of the coal sample was smaller, and the water content of the coal sample was relatively high. Under its comprehensive influence, the flammability was poor and the flammability index  $C$  was low. When the coal particle size was less than 18–35 mesh, the average pore diameter inside the coal body increased, and the oxygen migration between pores was more free. However, due to the influence of void fraction and other factors, the flammability index  $C$  increased first and then decreased, with the maximum value occurring for the D4 sample, and the value of  $C$  was 1.7 times that of the raw coal.

In combination with the flammability index  $C$ , the comprehensive combustion index  $S$  of water immersion coal samples with different sizes (Figure 6) and parameters were obtained through the infrared test. Infrared structural parameters  $I_1$ ,  $I_2$ , and  $I_3$ ; coal size  $P_s$ ; heating rate  $H_r$ ;  $C$ ; and  $S$  were analyzed using the least square method and stepwise regression analysis. The functional relationship was obtained using the SPSS software:

$$C \times 10^9 = 0.23H_r^2 - 4.64H_r + 0.012P_s \cdot H_r - 0.14P_s - 17.6724I_1^2 + 101.79I_1 - 56.61$$

with the correlation coefficient  $R^2$  was 0.977, and  $S \times 10^{12} = 0.37H_r^2 - 14.33H_r - 10310.18I_2 \cdot I_3 + 9237.92I_2 - 16290.08I_3 - 14490.69$ , with the correlation coefficient  $R^2$  was 0.906. It can be seen that the flammability index  $C$  was mainly affected by the  $H_r$ ,  $P_s$ , and  $I_1$ . The composite combustion index  $S$  was mainly affected by  $H_r$ ,  $I_2$ , and  $I_3$ .

**2.3.3. Kinetic Analysis of Oxidation Reaction.** Coal combustion is a very complex oxidation reaction process, and thus far, the specific combustion mechanism is not clear. To further explore the combustion mechanism of the water immersion coal, the Flynn–Wall–Ozawa (FWO) method was used to analyze the low-temperature oxidation reaction kinetics of the raw coal and water immersion coal samples with different particle sizes, and the relationship between the conversion rate of coal samples and the temperature change under different heating rates was obtained. Figure 7 shows the

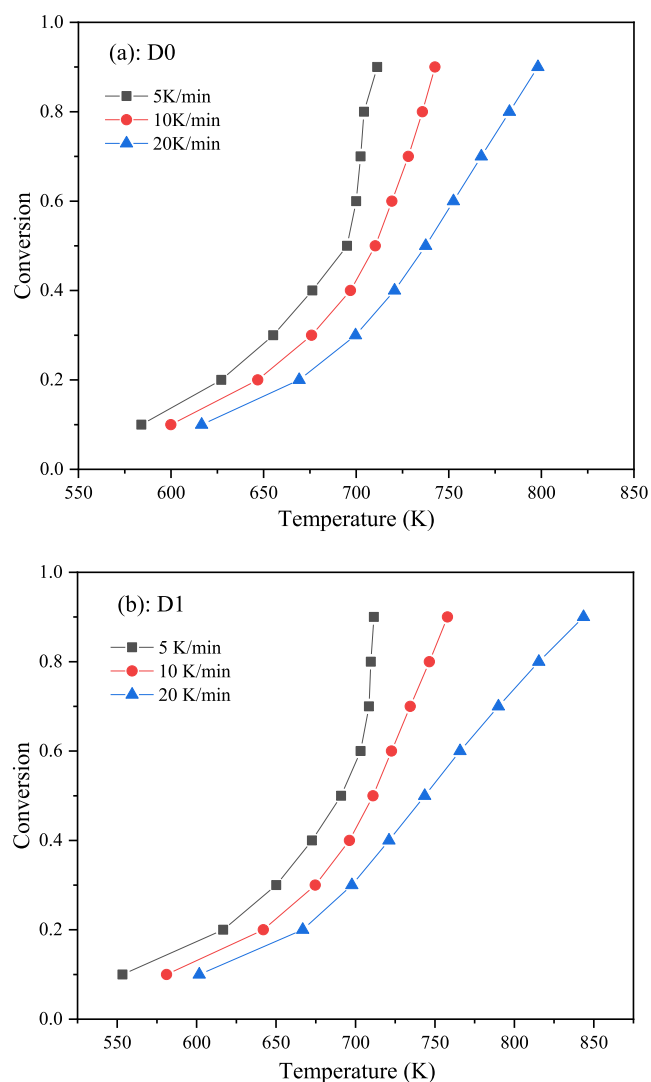


**Figure 7.** Relationship between conversion rate and temperature for the D0 and D1 coal samples at different heating rates.

relationship between the conversion rate and temperature of the D0 and D1 coal samples at different heating rates. It can be seen from Figure 7 that under the influence of heat transfer and heat release due to oxidation, under the same temperature conditions, the higher the heating rate was, the lower the conversion rate of the coal sample was, resulting in a lower corresponding temperature at the end of the coal oxidation reaction. This result is consistent with the results of previous research. In addition, for the water immersion coal samples with different particle sizes, under different heating rates, the initial temperatures of the oxidation reaction of the water immersion coal were significantly lower than those of the raw coal. This indicates that the reactivity of the water immersion coal was higher than that of the raw coal, and the water immersion coal was more prone to spontaneous combustion.

Figure 8 shows the relationship between  $\ln\beta$  and the temperature of the D0 and D1 coal samples at different conversion rates obtained via the FWO method. The linear regression equations under different conversion rates ( $\alpha$ ) were obtained via linear fitting of this relationship. The slope and intercept of the fitting equation are the apparent activation energy ( $E_a$ ) and pre-exponential factor ( $A_a$ ) of coal samples, respectively, and the relationship between the conversion rate

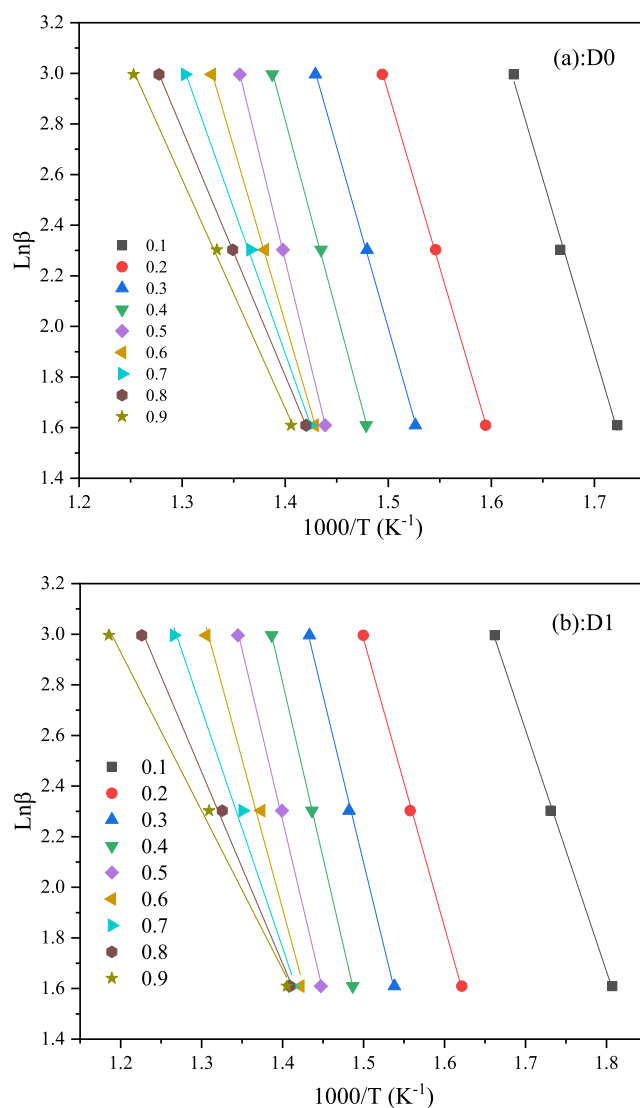


**Figure 8.** Relationship between  $\ln\beta$  and temperature for the D0 and D1 coal samples at different conversion rates.

and activation energy of the raw coal and water-saturated coal samples with different particle sizes is shown in Figure 9.

Based on the above results of the infrared spectrum analysis, low-temperature oxidation tests, and oxidation reaction kinetics of the water immersion coal samples and raw coal with different particle sizes, the water immersion process affected the physical and chemical structure of the coal. In addition, the immersion process resulted in the dissolution of the inorganic minerals in the coal, and the coal skeleton absorbed water, expanded, and softened, resulting in the secondary development of pore structures such as pore expansion. In addition, the contact area between the coal and oxygen and the oxygen supply channel increased, and the reaction rate between the active groups in the coal and the oxygen was accelerated. Moreover, the water immersion process increased the active group content of the coal and accelerated the coal-oxygen composite reaction. In terms of the chemical activity of the coal, the mechanism of reactive free radical reaction during the oxidation of immersed coal is shown in Figure 10. The size of the coal samples not only affected the pore development but also affected the voidage of coal samples, which further affected the formation of active

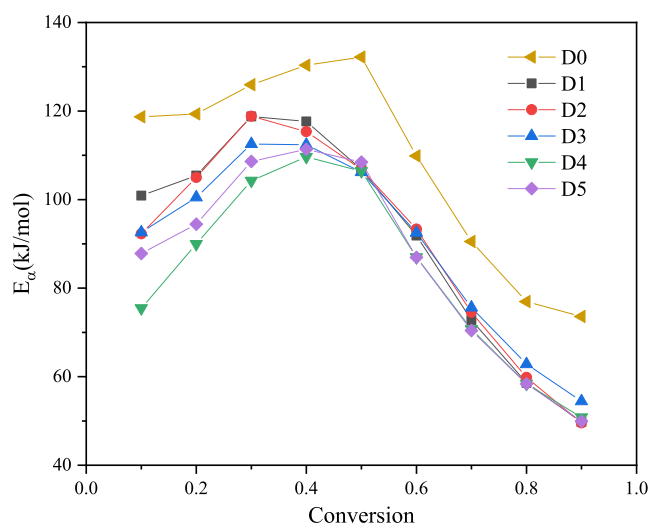


**Figure 9.** Relationship between conversion rate and activation energy for the raw coal and water immersion coal samples with different particle sizes.

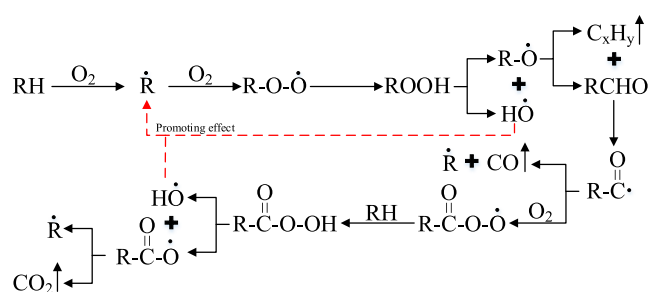


**Figure 10.** Mechanism of reactive free radical reaction during the oxidation of immersed coal.

functional groups such as hydroxyl and aromatic hydrocarbons in the process of coal immersion, and these functional groups reacted with the hydroxyl radicals and oxygen to form coal-oxygen complexes, which broke down into CO, CO<sub>2</sub>, C<sub>x</sub>H<sub>y</sub>, H<sub>2</sub>O, and new carbon radicals. These newly created carbon radicals participated in the coal oxidation process, and thus, the free radical chain reaction of the coal oxidation was accelerated.

### 3. CONCLUSIONS

In summary, in this study, the influences of coal groups and spontaneous combustion characteristics of coal samples of different sizes in the process of water immersion was investigated, relevant experimental studies were carried out, and the spontaneous combustion mechanism of coal samples of different sizes in the process of oxidation was discussed. The main conclusions were as follows.

- (1) The immersion process will further promote the dissolution of soluble substances in coal and promote the re-development of coal pore structure. The micro-pore volume and average pore diameter of the water immersion coal were 1.87–2.58 times and 1.02–1.13 times of the raw coal, respectively, and the specific surface area was reduced by 11.9–17.2% compared with the raw coal. The total pore volume of the water immersion coal was only 66.1–81.6% of that of the raw coal.

- (2) The content of the C=O, C–O, and –CH<sub>3</sub>/–CH<sub>2</sub>– groups in the water immersion coal decreased, while the content of the –OH functional groups increased. With the increased in the coal sample size, the content of the –OH functional groups decreased initially and then increased. The immersion process promoted the development of the pore structure of the coal samples, further enlarged the contact point between the active groups and oxygen in the coal samples, and promoted the formation of the –OH functional groups. The I<sub>1</sub>, I<sub>2</sub>, and I<sub>3</sub> values of the water immersion coal were 62.6–77.0, 39.2–83.9, and 102.3–107.7% of the raw coal, respectively. The reactivity of the water immersion coal was improved.

- (3) The characteristic temperature of coal samples under different heating rates was affected by water content, Hr, Ps, coal voidage, and other factors. With the combination of the least square method and stepwise regression analysis method, the function expression of the ignition point temperature, flammability index C, and comprehensive combustion index S of the coal samples immersed in water were obtained as follows:  $T_g = 4.35Hr + 79.02I_2 + 4.06Ps \cdot I_2 - 6.42Ps + 266.95$ ,  $C \times 10^9 = 0.23Hr^2 - 4.64Hr + 0.012Ps \cdot Hr - 0.14Ps$ ,  $S \times 10^{12} = 0.37Hr^2 - 14.33Hr - 10310.18I_2 \cdot I_3 + 9237.92I_2 - 16290.08I_3 - 14490.69$ , and the correlation coefficients R<sub>2</sub> were 0.936, 0.977, and 0.906, respectively.

- (4) The apparent activation energy of water immersion coal samples was lower than that of raw coal samples, and the average apparent activation energy of the water immersion coal of different sizes decreased by 12.4–19.7%, and the apparent activation energy of coal sample with size of 60–120 mesh was the lowest on the whole. The influence of immersion process on coal samples of different particle sizes was within the conversion range of 0.1–0.5, indicating that the apparent activation energy in the low-temperature oxidation stage was significantly different. The activity of the water immersion coal was significantly increased, and it was more prone to oxidation and spontaneous combustion.

## 4. EXPERIMENTS AND METHODS

**4.1. Coal Sample Selection and Preparation.** The experimental coal was from the Fengshuigou Coal Mine operated by Pingzhuang Coal Company in Inner Mongolia. A large piece of fresh coal was wrapped with plastic and transported to the laboratory, where its surface was peeled off, its central part was removed, and parts of it were crushed and ground. The raw coal (120–200 mesh) was numbered D0. The 8–18, 18–35, 35–60, 60–120, and 120–200 mesh coal samples were numbered D1–D5, which were immersed in deionized water for 60 days, and then the water immersion coal samples were removed from the water. The water immersion coal samples were evenly spread in the evaporating dish and naturally dried for 72 h under laboratory conditions. Meanwhile, fresh raw coal was also treated under the same conditions. Before the experiment, the coal sample was dried in a vacuum drying oven at 40 °C for 48 h to eliminate the influence of external moisture on the experimental results.

Proximate analysis and elemental analysis of experimental coal samples were conducted in accordance with Chinese

Table 6. Proximate and Ultimate Analyses of Coal Samples

coal samples	proximate analysis (%)				ultimate analysis (%)				
	M (ad)	A (ad)	V (ad)	FC (ad)	C (daf)	H (daf)	O (daf)	N (daf)	S (daf)
D0	12.06	9.15	33.13	44.81	81.66	5.66	10.31	0.78	1.59
D1	11.88	9.19	34.15	46.29	81.70	5.58	10.28	0.81	1.63
D2	10.24	8.91	35.27	45.05	81.74	5.55	10.27	0.79	1.65
D3	9.52	8.87	35.42	44.94	81.78	5.42	10.24	0.79	1.77
D4	9.92	8.55	36.75	43.61	81.75	5.38	10.24	0.78	1.85
D5	9.92	8.18	38.11	42.98	81.77	5.39	10.22	0.73	1.89

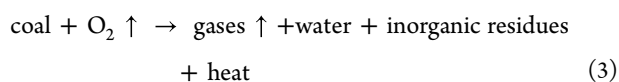
national standards GB/T212-2008 and GB/T31391, and the test results are shown in Table 6.

**4.2. Low-Temperature Nitrogen Adsorption Experiment of Coal Sample.** Considering the moisture and adsorbed gas contained in the coal sample itself, the coal sample was heated in a 105 °C vacuum for 5 h before the test, then degassed and cooled to room temperature. Next, the specific surface area and pore diameter of the coal sample were tested using the American MacasAP2020 automatic specific surface and pore diameter analyzer. Using N<sub>2</sub> as adsorption gas, the low-temperature nitrogen adsorption test was conducted at 77 K (liquid nitrogen temperature).

**4.3. Thermal Gravimetric-Differential Thermal Gravimetric Analysis of Coal Samples.** Considering the extremely complex physical and chemical properties of the coal itself, in this experiment, a synchronous thermal analyzer-differential scanning calorimeter (STA-DSC, NESCH, Germany) was used to conduct the analysis. Approximately 10 mg of the test sample was weighed and placed in a corundum crucible for heating. The heating rate of the experiment was 5, 10, 20 K/min, the heating range was 30–600 °C, the reaction gas was atmosphere (O<sub>2</sub> volume fraction of 21%; N<sub>2</sub> volume fraction of 79%), and the flow rate of dry air was 100 mL/min.

**4.4. Fourier Infrared Spectroscopy Analysis of Coal Samples.** Currently, infrared spectroscopy is a commonly used method to test the various and relative contents of the functional groups in coal samples. In this experiment, a Fourier transform infrared spectrometer (Bruker Company, Germany) was used to analyze the functional group changes in the raw coal and water immersion coal samples with different particle sizes. Before the test, the coal samples were dried in a vacuum drying oven at 110 °C for 48 h and cooled to room temperature. The experimental coal samples were thoroughly ground and crushed, and the fully ground samples were mixed with dry KBr analytical reagent in a ratio of 1:100. The mixture was placed in a mold and subjected to a pressure of 10 MPa for 60 s. The obtained sample was placed in the instrument for spectral analysis. The wave number scanning range was 4000–400 cm<sup>-1</sup>, the acquisition frequency was 30 s/time, and the spectrum was scanned 89 times. Before each experiment, a blank background spectrogram was obtained, and the infrared spectral data obtained were smoothed and baseline corrected.

**4.5. Kinetic Analysis of Coal Sample Oxidation Process.** Coal is a complex mixture of organic matter and inorganic matter. In the oxidation process, coal reacts with oxygen to generate multi-component gas and water and releases heat



In the process of coal pyrolysis, according to the measured TG curve, the mass loss reaction conversion rate of the coal sample can be calculated as follows

$$\alpha = \frac{m_0 - m_t}{m_0 - m_\infty} \quad (4)$$

where  $\alpha$  is the conversion rate, and  $m_0$ ,  $m_t$ , and  $m_\infty$  are the initial mass of the coal sample, the mass at time  $t$ , and the residual mass of the sample (mg), respectively.

According to the reaction rate formula, the oxidation reaction rate of coal at any temperature is

$$\frac{d\alpha}{dt} = k(T) \times f(\alpha) \quad (5)$$

where  $d\alpha/dt$  is the reaction rate,  $k(T)$  is the pyrolysis rate constant,  $t$  is the reaction time (min), and  $T$  is the reaction temperature (K).

According to the Arrhenius equation

$$k(T) = A \cdot \exp\left(-\frac{E}{RT}\right) \quad (6)$$

where  $A$  is the pre-exponential factor (min<sup>-1</sup>),  $E$  is the reaction activation energy (KJ/mol), and  $R$  is the universal gas constant [8.314 J/(mol·K)].

By substituting eqs 6 into 5, the following equation can be obtained

$$\frac{d\alpha}{dt} = A \cdot \exp\left(-\frac{E}{RT}\right) \times f(\alpha) \quad (7)$$

For a non-isothermal process, when the heating rate  $\beta$  ( $\beta = dT/dt$ ) is constant, the reaction rate can be expressed as

$$\frac{d\alpha}{dT} = \frac{A}{\beta} \cdot \exp\left(-\frac{E}{RT}\right) \times f(\alpha) \quad (8)$$

Then, the integral form of the function  $f(\alpha)$  is

$$g(\alpha) = \int_0^\alpha \frac{d\alpha}{f(\alpha)} = \frac{A}{\beta} \int_{T_0}^T \exp\left(-\frac{E}{RT}\right) dT \quad (9)$$

where  $T_0$  is the initial reaction temperature.

Because the FWO method does not need to assume the reaction mechanism, the model has good stability and reliability and has been widely used in the field of pyrolysis kinetic analysis of complex reactions. Thus, this model is considered to be more suitable for the kinetic study of coal samples.<sup>33</sup> Therefore, the FWO model was used in this study to analyze the kinetic characteristics of the water immersion coal samples and the raw coal samples with different particle sizes during the oxidation process. The expression of the FWO method is as follows

$$\ln(\beta) = \ln \frac{A_{\alpha} E_{\alpha}}{Rg(\alpha)} - 5.331 - 1.052 \frac{E_{\alpha}}{RT_{\alpha}} \quad (10)$$

where  $A_{\alpha}$ ,  $E_{\alpha}$ , and  $T_{\alpha}$  are the corresponding pre-exponential factor, activation energy, and temperature when the conversion rate is  $\alpha$ , respectively.

Finally, through linear fitting, the slope and intercept obtained correspond to the activation energy and pre-exponential factor at a certain conversion rate, respectively.

## AUTHOR INFORMATION

### Corresponding Author

Zikun Pi – School of Safety and Management Engineering, Hunan Institute of Technology, Hengyang, Hunan 421002, China; [orcid.org/0000-0003-3902-8150](https://orcid.org/0000-0003-3902-8150); Email: 496492248@qq.com

### Authors

Rui Li – School of Safety and Management Engineering, Hunan Institute of Technology, Hengyang, Hunan 421002, China

Wei Guo – College of Safety Science and Engineering, Liaoning Technical University, Fuxin, Liaoning 123000, China

Xiaoli Liu – The State Key Laboratory of Hydrosience and Engineering Tsinghua University, Beijing 100084, China

Zhenya Zhang – School of Safety Engineering, Ningbo University of Technology, Ningbo, Zhejiang 315211, China; Zhejiang Institute of Tianjin University, Ningbo, Zhejiang 315211, China

Yan Wang – Inner Mongolia Autonomous Region Emergency Management Technology Center, Hohhot, Inner Mongolia 010000, China

Yifu Zhang – School of Safety and Management Engineering, Hunan Institute of Technology, Hengyang, Hunan 421002, China

Guangkuo Yin – School of Safety and Management Engineering, Hunan Institute of Technology, Hengyang, Hunan 421002, China

Xue Li – School of Safety and Management Engineering, Hunan Institute of Technology, Hengyang, Hunan 421002, China

Complete contact information is available at:

<https://pubs.acs.org/10.1021/acsomega.3c00109>

### Funding

This research was funded by the National Natural Science Foundation of China (grant number 51804107), the Natural Science Foundation of Hunan Province (grant numbers 2020JJ4260 and 2021JJ30206), and the Key Projects of Hunan Education Department (grant number 19A123), and the Innovation and Entrepreneurship Training Project for College students in Hunan Province (grant numbers S202211528091 and S202211528095), and Open Research Fund Program of State key Laboratory of Hydrosience and Engineering (grant number sklhse-2021-D-01).

### Notes

The authors declare no competing financial interest.

## ACKNOWLEDGMENTS

The results of this study could not have been possible without the efforts of the staff on the research team, and at the same time, we sincerely thank the editors and reviewers for spending their valuable time reviewing and providing valuable com-

ments. We thank LetPub ([www.letpub.com](http://www.letpub.com)) for its linguistic assistance during the preparation of this manuscript.

## REFERENCES

- Onifade, M. Countermeasures against coal spontaneous combustion: a review. *Int. J. Coal Prep. Util.* **2022**, *42*, 2953–2975.
- Ulyanova, E. V.; Malinnikova, O. N.; Dokuchaeva, A. I.; Pashichev, B. N. Effect of Structural Nonuniformity on Spontaneous Combustion Liability of Coal. *Solid Fuel Chem.* **2022**, *56*, 426–431.
- Xu, Q.; Yang, S. Q.; Yang, W. M.; Tang, Z. Q.; Hu, X.; Song, W.; Zhou, B. Micro-structure of crushed coal with different metamorphic degrees and its low-temperature oxidation. *Process Saf. Environ. Protect.* **2020**, *140*, 330–338.
- Zhang, X.-Y.; Zhang, Y.-L.; Wang, J.-F.; Hao, H.-D.; Wu, Y.-G.; Zhou, C.-S. Study on the effect and mechanism of foreign moisture on coal spontaneous combustion. *J. Fuel Chem. Technol.* **2020**, *48*, 1–10.
- Wang, J.; Zhang, Y.; Wang, J.; Zhou, C.; Wu, Y.; Tang, Y. Study on the Chemical Inhibition Mechanism of DBHA on Free Radical Reaction during Spontaneous Combustion of Coal. *Energy Fuels* **2020**, *34*, 6355–6366.
- Zhang, D. S.; Fan, G. W.; Zhang, S. Z.; Ma, L. Q.; Wang, X. F. Equivalent water-resisting overburden thickness for water-conservation mining: Conception, method and application. *J. China Coal Soc.* **2022**, *47*, 128–136.
- Xing, Y. L.; Zhao, Q. K. Evaluation on Sealing-Opening of Working Face under Closed Distance Seam Group and Influence Degree of Surface Crack. *Coal Technol.* **2021**, *40*, 144–148.
- Zhu, M. T.; Li, B.; Liu, G. Groundwater risk assessment of abandoned mines based on pressure-state-response—The example of an abandoned mine in southwest China. *Energ. Rep.* **2022**, *8*, 10728–10740.
- Yang, S.; Li, X. H.; Wang, J.; Yang, S. H.; Shen, Z.; Xu, G. Z. Study on Pressure Relief Technology of High-Pressure Water Jet of Residual Coal Pillar in Overlying Goaf in Close Seam Mining. *Shock Vib.* **2022**, *2022*, 7842921.
- Bu, Y. C.; Niu, H. Y.; Wang, H. Y.; Qiu, T.; Chen, H. Y.; Xue, D. Characteristics of lean oxygen combustion and dynamic micro-reaction process of water-soaked coal. *Fuel* **2023**, *332*, 126010.
- Hu, Q. T.; Zhang, Y. B.; Li, Q. G.; Cao, J.; Song, M. Y.; Hu, L. P.; Liu, J. C.; Deng, Y. Z.; Shi, J. L.; Zheng, X. W. Experimental research on progressive failure characteristics of water-immersed coal: Implications for hydraulic fracturing. *Eng. Geol.* **2022**, *308*, 106809.
- Zhang, L.; Zhang, W. C. Influence of immersion time on initial spontaneous combustion characteristics of immersed air-dried coal. *Coal Eng.* **2021**, *53*, 136–139.
- Cunbao, D.; Ling, Q.; Xuefeng, W.; Fengwei, D.; Xun, Z. Spontaneous combustion characteristics and infrared analysis of soaked lignite. *China Saf. Sci. J.* **2018**, *28*, 105–110.
- Ma, B. C.; Chen, Y. Q.; Yang, Y. L.; Xu, S. M.; Zhu, Y. An Experimental Study on Impact of Soaking Time on Low Temperature Oxidation Characteristics of Coal. *Saf. Coal Mine* **2016**, *47*, 18–21.
- Zhao, X. G.; Dai, G. L. Experimental study on spontaneous combustion characteristics of oxidized coal. *J. Saf. Sci. Techno.* **2020**, *16*, 55–60.
- Wen, H.; Lu, Y. B.; Liu, W. Y. Experimental study on the risk of secondary oxidation spontaneous combustion of water immersed coal. *Min. Saf. Environ. Prot.* **2020**, *47*, 6–11.
- Sensogut, C.; Ozdeniz, A. H.; Gundogdu, I. B. Temperature profiles of coal stockpiles. *Energy Sources, Part A* **2008**, *30*, 339–348.
- Zhao, H.; Yu, J. L.; Liu, J. S.; Tahmasebi, A. Experimental study on the self-heating characteristics of Indonesian lignite during low temperature oxidation. *Fuel* **2015**, *150*, 55–63.
- Yang, M.; Liu, L.; Liu, J. J.; Mao, J. R.; Chai, P. Study on joint characterization of pore structure of middle-rank coal by nitrogen adsorption-mercury intrusion-NMR. *Coal Sci. Technol.* **2021**, *49*, 67–74.
- Zhu, J.; Zhang, B.; Wang, Q. Q.; Jiang, Y. D.; He, F. The interdependency of pore structures and coal dynamic failures. *J. China Univ. Min. Technol.* **2018**, *47*, 97–103.

- (21) Liu, Z. X.; Ye, C.; Shi, F.; Guo, Y. W. Numerical simulation for the microscopic mechanical features of the heterogeneous coal samples based on the biaxial compression. *J. Saf. Environ.* **2021**, *21*, 179–186.
- (22) Cetin, E.; Gupta, R.; Moghtaderi, B. Effect of pyrolysis pressure and heating rate on radiata pine char structure and apparent gasification reactivity. *Fuel* **2005**, *84*, 1328–1334.
- (23) Choi, H.; Thirupathiraja, C.; Kim, S.; Rhim, Y.; Lim, J.; Lee, S. Moisture Readsorption and Low Temperature Oxidation Characteristics of Upgraded Low Rank Coal. *Fuel Process. Technol.* **2011**, *92*, 2005–2010.
- (24) Smith, I. W. The combustion rates of coal chars: a review. *Symp. (Int.) Combust.* **1982**, *19*, 1045–1065.
- (25) Dereppe, J. M.; Moreaux, C.; Landais, P.; Monthieux, M. Study of the artificial oxidation of a humic coal by  $^{13}\text{C}$  CP/MAS nuclear magnetic resonance. *Fuel* **1987**, *66*, 594–599.
- (26) Fry, R.; Day, S.; Sakurovs, R. Moisture-induced swelling of coal. *Int. J. Coal Prep. Util.* **2009**, *29*, 298–316.
- (27) Song, S.; Qin, B. T.; Xin, H. H.; Qin, X. W.; Chen, K. Exploring effect of water immersion on the structure and low-temperature oxidation of coal: A case study of Shendong long flame coal, China. *Fuel* **2018**, *234*, 732–737.
- (28) Zhai, X.; Ge, H.; Wang, T.; Shu, C.-M.; Li, J. Effect of water immersion on active functional groups and characteristic temperatures of bituminous coal. *Energy* **2020**, *205*, 118076.
- (29) Dong, Z. W.; Yu, W. H.; Jia, T. G.; Guo, S. L.; Geng, W. L.; Peng, B. Experimental Study on the Variation of Surface Widths of Lignite Desiccation Cracks during Low-Temperature Drying. *ACS Omega* **2021**, *6*, 19409–19418.
- (30) Wang, K.; Liu, X. R.; Deng, J.; Zhang, Y. N.; Jiang, S. R. Effects of pre-oxidation temperature on coal secondary spontaneous combustion. *J. Therm. Anal. Calorim.* **2019**, *138*, 1363–1370.
- (31) Wen, G. C.; Yang, S.; Liu, Y. B.; Wu, W. B.; Sun, D. L.; Wang, K. Influence of water soaking on swelling and micro-characteristics of coal. *Energy Sci. Eng.* **2020**, *8*, 50–60.
- (32) Zheng, K. Y.; Yang, Y. L.; Miao, G. D.; Li, P. R. Influencing Mechanism of Water Soaking Process on Spontaneous Combustion Characteristics of Goaf Residual. *Coa. J. Combust. Sci. Technol.* **2021**, *27*, 665–674.
- (33) Zhong, X. X.; Kan, L.; Xin, H. H.; Qin, B. T.; Dou, G. L. Thermal effects and active group differentiation of low-rank coal during low-temperature oxidation under vacuum drying after water immersion. *Fuel* **2019**, *236*, 1204–1212.
- (34) Guo, S. L.; Yan, Z.; Yuan, S. J.; Geng, W. L. Inhibitory effect and mechanism of L-ascorbic acid combined with tea polyphenols on coal spontaneous combustion. *Energy* **2021**, *229*, 120651.
- (35) Zhang, J. L.; Ruan, G. Y.; Wang, M. M. Study on the influence of immersion degree on coal spontaneous combustion characteristics. *China Min. Mag.* **2022**, *31*, 132–139.
- (36) Li, M.-F.; Zeng, F.-G.; Qi, F.-H.; Sun, B.-L. Raman Spectroscopic Characteristics of Different Rank Coals and the Relation with XRD Structural Parameters. *Spectrosc. Spect. Anal.* **2009**, *29*, 2446–2449.
- (37) Guo, H. Y.; Li, S. S.; Shen, Y.; Li, Y. S.; Xu, X. K.; Liu, X. L. Variation characteristics of the structure and biological gas production effect of coal with different weathering degrees. *J. Saf. Environ.* **2022**, *22*, 1510–1517.
- (38) Qin, B. T.; Song, S.; Qi, X. Y.; Zhong, X. X.; Liu, C. Effect of soaking process on spontaneous combustion characteristics of long-flame coal. *J. China Coal Soc.* **2018**, *43*, 1350–1357.
- (39) Pi, Z. K.; Dong, Z. W.; Li, R.; Wang, Y.; Li, G. L.; Zhang, Y. F.; Peng, B.; Meng, L. P.; Fu, S. Y.; Yin, G. K. Low-Field NMR Experimental Study on the Effect of Confining Pressure on the Porous Structure and Connectivity of High-Rank Coal. *ACS Omega* **2022**, *7*, 14283–14290.
- (40) Lu, W.; Li, J.; Li, J.; He, Q.; Hao, W.; Li, Z. Oxidative kinetic characteristics of dried soaked coal and its related spontaneous combustion mechanism. *Fuel* **2021**, *305*, 121626.
- (41) Wang, H. Y.; Fan, S. W.; Yao, H. F. FTIR Analysis on Surface Chemical Structure of Two Different Degrees of Metamorphic Coal. *Saf. Coal Mine* **2018**, *49*, 194–197.
- (42) Han, F.; Zhang, Y. G.; Meng, A. H.; Li, Q. H. FTIR analysis of Yunnan Lignite. *J. China Coal Soc.* **2014**, *39*, 2293–2299.
- (43) Si, W. B.; Wang, D. M. Experimental study on effect of sulfur on spontaneous combustion process of long-flame coal. *Coal Sci. Technol.* **2020**, *48*, 103–107.
- (44) Jiang, P.; Sun, W. Q.; Li, Z. B.; Liao, R.; Li, L.; Liao, Q. Y. Stage inhibition characteristics of composite inhibitor in process of inhibiting coal spontaneous combustion. *Coal Sci. Technol.* **2022**, *50*, 68–75.
- (45) Zhao, J. W.; Wang, W. C.; Fu, P.; Wang, J. L.; Gao, F.; Xue, P. F. Experimental study on influence of water immersion and air-drying process on coal spontaneous combustion characteristics. *Saf. Coal Mine* **2022**, *53*, 37–43.
- (46) Wen, H.; Liu, C.; Zhao, Q. W.; Wang, Z. P.; Lu, Y. B.; Dai, A. P.; Zhang, D. Study on thermal reaction kinetics of long flame coal spontaneous combustion in Tangjiahui Mine. *Saf. Coal Mines* **2022**, *53*, 129–136.
- (47) Wang, T. Y.; Wang, J. Z.; Han, M.; Niu, J. G.; Wang, W. F.; Zhang, D. Influence of heating rate on coal spontaneous combustion characteristics in Tangkou Coal Mine. *Shaanxi Coal* **2022**, *41*, 23–26.
- (48) (a) Liu, J. Y.; Fu, J. W.; Sun, S. Y.; Zhuo, Z. X.; Kuo, J. H.; Sun, J.; Wang, Y. J.; Li, X. Y. Co-combustion of various sources of sludge and its combustion performance. *J. Environ. Sci. China* **2016**, *36*, 940–952. (b) Zhang, Y.; Zhao, W.; Wu, H.; He, Z.; Qian, Y.; Lu, X. Performance, combustion, and emission evaluation of ethanol-gasoline blends ignited by diesel in dual-fuel intelligent charge compression ignition (ICCI) engine. *J. Energy Resour. Technol.* **2022**, *144*, 082104.
- (49) Jin, Y. F.; Li, Q. Z.; Liu, Y. Study on Characteristic Parameters of Coal Spontaneous Combustion and Variation Characteristics of Free Radicals. *Coal Technol.* **2022**, *41*, 101–104.
- (50) Feng, H.; Zuo, C. B.; Wang, B. F.; Yan, W.; Cao, J. Y. Analysis of Combustion Characteristics of Coal Mixed Gangue under Different Heating Rates. *Energy & Energy Conservation* **2018**, *4*, 20–22.
- (51) Shao, Y.; You, F.; You, M. W.; Xu, Y. Q. Effect of the oxygen content and heating rate on the oxidation process of the long-flame burning coal. *J. Saf. Environ.* **2016**, *16*, 177–181.